JOURNAL OF OPTOELECTRONICS AND ADVANCED MATERIALS Vol. 16, No. 11-12, November - December 2014, p. 1344 - 1350

Gold mediated ZnO nanostructure layers on Si surface by continuous spray pyrolysis with their optical properties

H. DHASMANA[a,b], V. DUTTA[a]
[a]*Photovoltaic Laboratory, Centre for energy studies, Indian Institute of Technology, Delhi-110016*
[b]*Department of Applied Science, Echelon Institute of Technology, Faridabad-121001*

The growth of ZnO nanostructure layers mediated by Au nanoparticles and thin film on Si surface are performed by continuous spray pyrolysis reactor using Zinc solution seed layer. XRD data suggests Au nanoparticles size dependent role in ZnO growth. SEM and PL measurement confirm enhancement in the surface coverage of ZnO nanorods growth, better optical quality of thin film with enhanced uniformity in nanorods size for larger Au nanoparticle mediated ZnO deposition. The chlorine incorporation in ZnO thin film due to seed layer content is removed by the presence of Erbium in the precursor solution. The reflectance show higher surface plasmon resonance and significant light reduction up to 54.7 % of existing reflectance in 300-1200 nm wavelength regions for larger size Au nanoparticles which may be helpful in the increase of photocurrent in Si solar cells.

(Received November 11, 2013; accepted November 13, 2014)

Keywords: ZnO nanorods, Plasmonic effect, Au nanoparticles, Continuous Spray Pyrolysis

1. Introduction

In a crystalline silicon (Si) solar cell, the efficiency of the device can be increased by optical coupling of incident light on Si surface. The optical reflection losses from the surface are critical in determining the ultimate efficiency of Si solar cell and account for ~ 5% efficiency reduction [1].The surface texturization and antireflection coating help in reducing the reflection loss [2]. A 42.7% reduction of reflected light can result in the enhancement of Si solar cell efficiency by 112.4% [3].The light suppression by nanostructure layers has gained popularity for devices like Si solar cells and can enhance efficiency by the way of increasing photocurrent. Surface plasmonic effects using gold (Au) and silver (Ag) nanoparticles (NPs) have also given rise to improved performance. Since Zinc Oxide (ZnO) nanostructures can be formed on Si surface using a seed layer, Au NPs as seed layer can assist the ZnO nanostructure growth as well as give rise to the surface plasmonic effects. The phenomenon of Localized Surface Plasmon Resonance (LSPR) can occur and help improve the Si solar cell performance [4-5]. The resonance wavelength depends on the NPs size, shape, and local dielectric environment [6-7]. Recent studies suggest surface plasmonic effect of Au NPs with ZnO material for different applications but very limited work is dedicated on this material combination for Si solar cell applications [8-11].

Zinc Oxide (ZnO) has inherent material properties such as good transparency in visible wavelength region, appropriate refractive index (nearly 2), ability to form textured coating via anisotropic growth, good chemical stability etc. Therefore, ZnO can play a useful role in Si solar cell as antireflection [12-13] and passivation layer [14]. Recently, ZnO nanorods array has enhanced 3 % of Si solar cell efficiency by the way of increasing photocurrent due to light suppression on Si surface [15]. ZnO nanostructure such as porous particles is also reported for minimizing reflection loss [16]. The growth of controllable ZnO nanostructure on Si surface can be achieved by gas phase synthesis methods [17-18]. But these techniques involve sophisticated equipments with rigorous experimental conditions which make difficult technological incorporation of these methods in existing Si solar cell device fabrication line. Therefore, a simple inline process to create ZnO nanostructures on Si surface will be useful for industrial applications.

The continuous spray pyrolysis (CoSP) reactor includes all the additional features such as simple, vacuum less, fast etc and has been established in the lab for fabricating NPs as well as nanostructure layers on glass [19]. The addition of Au NPs in ZnO nanostructure growth has been studied by various research groups and is

suggested for its role as a seed layer and catalytic layer in the ZnO growth [20-23]. It is expected that additional LSPR and seed layer effect of Au NPs in ZnO growth may be helpful in light reduction and hence increase efficiency of Si solar cell via increase of photocurrent. The paper reports size dependent Au particles as well as Au thin film mediated ZnO growth on Si surface by CoSP reactor and the reflection study suggests a better light coupling does become possible. Further an attempt has been made to explore lanthanide doping in precursor solution by Erbium (Er) ions in 40 nm Au NPs mediated ZnO growth.

2. Experimental Section

The experimental set up of CoSP reactor consists of three zones i.e. evaporation, spray and deposition zone. After solvent evaporation of spray droplets at 550^0C in first zone, spray pyrolysis occurs in second zone at high temperature 850^0C and self assembly of spray pyrolysed NPs takes place in third zone through thermophoresis [24] at 550^0C. All the substrate chosen for deposition were single side polished boron doped p-type (100) Si substrate with resistivity 1-10 ohm-cm, thickness 380 µm. These substrates were cleaned in piranha solution along with ultrasonification in Isopropyl alcohol, acetone and DI water. Colloidal Au NPs were synthesized by reported chemical reduction method [25].These Au NPs are spray deposited on Si surface at 120^0C. For Au thin film on Si surface, Au with a mass thickness of 1.3 nm (approximate film thickness in 8 – 10 nm range) was deposited by thermal evaporation onto Si surface. The Zn solution seed layer was prepared by dissolving 0.1 M Zinc chloride in 20 ml methanol. The Au mediated and bare Si substrate were immersed in this solution for 5-7 minutes and then dried in air at 120^0C for 2 minutes. To prepare Zinc acetate (ZA) precursor solution, 0.1 M Zinc acetate dihydrate (Sigma- Aldrich 98% pure) was dissolved in 100 ml distilled water and kept for stirring until it changes to the transparent solution. The solution flow rate and gas pressure were kept constant at 2 ml/min and 2.2 kgf/cm^2 for 2 minutes deposition time with nitrogen as carrier gas in all the cases. These seed layer solution mediated Si surfaces were then undergone for spray pyrolysis in CoSP reactor under various deposition conditions. Erbium pentahydrate (Sigma Aldrich) was used as a source dopant in ZA precursor solution for 1% atomic weight Er ions concentration.

The crystal structure and surface morphology of ZnO nanostructures over (100) Si surface were investigated by Philips XPERT PRO (PW3040) X-Ray Diffractometer (XRD) and ZEISS EVO-50 model Scanning Electron Microscope (SEM). Shape and size of Au NPs were assessed by Philips CM-12 transmission electron microscopy (TEM). Optical reflectance spectra in the wavelength region 300-1200 nm and UV-Visible absorption spectrum were obtained using Perkin-Elmer Lambda-1050 spectrophotometer. Photoluminescence (PL) study of

ZnO nanostructure thin films were investigated by Perkin Elmer Fluorescence spectrophotometer model LS 55.

Table 1.Sample details of ZnO nanostructure on polished Si surface

Sample details	Sample name
ZnO growth on Si surface with Zn solution seed layer only	Z/Si
ZnO growth on Si surface with Zn solution seed layer mediated by 15 nm Au particles	Au_15
ZnO growth on Si surface with Zn solution seed layer mediated by 40 nm Au particles	Au_40
ZnO growth on Si surface with Zn solution seed layer mediated by 40 nm Au particles for Er doped precursor solution.	Au_40Er
ZnO growth on Si surface with Zn solution seed layer mediated by Au thin film of mass thickness 1.3 nm.	Au_1.3
Bare polished Si surface	Si surface
Only mass thickness of 1.3 nm Au film on Si surface	Au_film/Si
Only spray deposited 40 nm Au particles on Si surface	40 nm Au NPs/Si
Only spray deposited 15 nm Au particles on Si surface	15 nm Au NPs/Si

3. Results and discussions

3.1. Characterization of Au particles

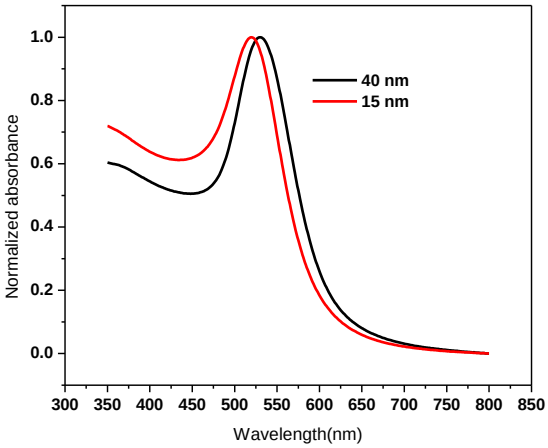

Fig. 1. Absorbance spectrum of 15 and 40 nm Au NPs .

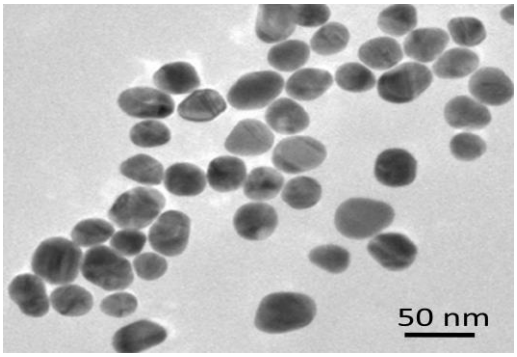

Fig. 2 TEM image of 40 nm Au NPs.

Fig. 1 shows UV-Visible absorbance `spectrum of 15 and 40 nm Au particles with corresponding absorban-ce peaks at 519 and 530 nm respectively with almost zero absorbance in above 700 nm wavelength region. Shape and size of Au NPs are confirmed with TEM measurement of 40 nm Au NPs shown in Fig. 2, which depicts Au NPs shape as nearly spherical.

3.2. Structural analysis

Fig. 3 shows index matched XRD pattern (JCPDS, File No. 36-1451) of ZnO nanostructure layers for 3 samples Z/Si, Au_15 and Au_40. For Z/Si, XRD depicts all corresponding peaks in Fig. 4 (a) with dominant (101) peak. In the case of Au_15, (002) oriented ZnO growth is observed (Fig. 4 (b)) and no extra Au peaks are observed in the spectrum. The role of Au NPs layer for ZnO growth is changed in the case of Au_40 and is confirmed with the presence of matching corresponding extra Au fcc peaks (JCPDS, File No. 4-0784) in Fig. 4 (c).

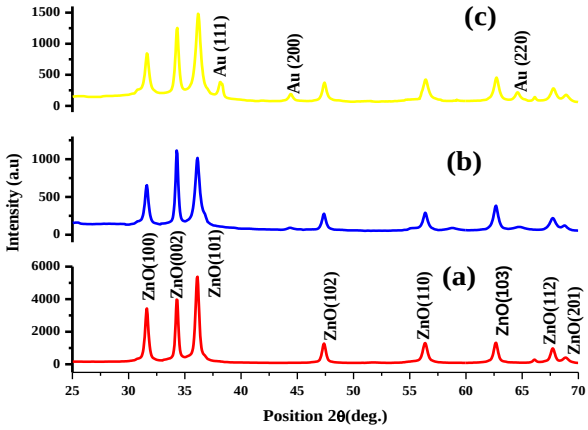

Fig. 3 *XRD pattern for (a)pure ZnO on Si (Z/Si) (b)15 nm (Au_15) and (c) 40 nm (Au_ 40) Au NPs mediated ZnO growth.*

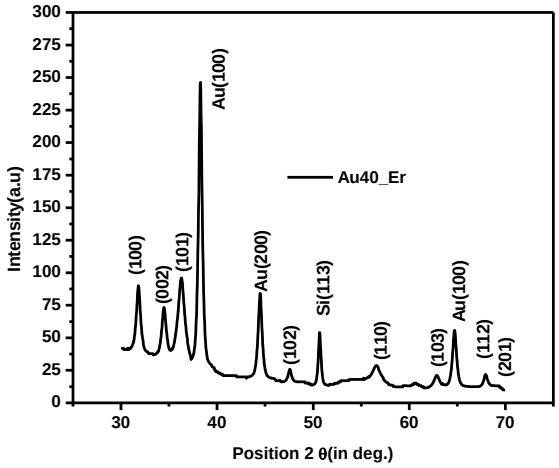

Fig. 4 XRD pattern of 40 nm Au NPs mediated ZnO growth with Er doped precursor solution (Au_40Er).

Fig. 4 depicts XRD of 40 nm Au NPs mediated ZnO growth with Er doped precursor solution. This Fig. shows dominant Au fcc peaks with respect to ZnO and Si peaks, which may be attributed to lower ZnO growth.

3.3. Surface study

Fig. 5 (a) shows the formation of multibranched nanorods on Si surface for Z/Si. Zinc (Zn) solution seed layer promotes nanorod growth, but it does not lead to vertically aligned nanorods, may be because of low deposition time. These shapes of nanorods are irregular and a large size variation amongst nanorods is observed. Surface morphology of ZnO growth on Zn solution seed layer mediated by thin Au film with mass thickness 1.3 nm is shown in Fig. 5 (b), which depicts no ZnO nanorods formation in the growth. But if the ZnO deposition is performed on different sizes of Au particles such as 15 nm and 40 nm along with Zn solution seed layer, the ZnO film growth profile is changed for the same deposition

condition of CoSP reactor. In the case of ZnO growth for Au_15, coalescence amongst nanorods starts and increased surface area coverage is also seen in Fig. 5 (c). This changed growth profile may be attributed to changed roughness profile due to the presence of Au NPs. In the case of Au_40, an active participation of Au NPs as seed layer in ZnO growth increases Si surface area coverage and also the coalescence amongst nanorods. More uniform ZnO nanorods of sizes ~150 nm are observed in Fig. 5 (d).

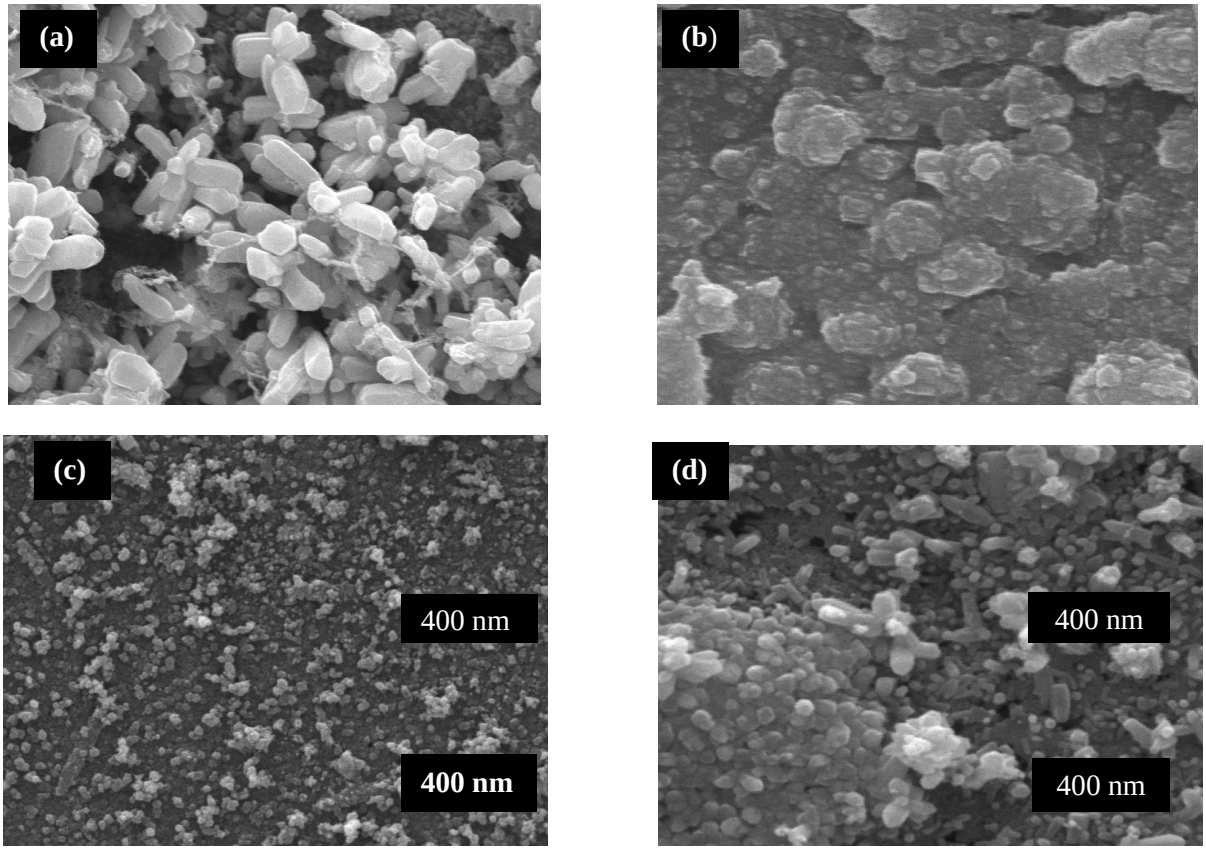

Fig. 5. SEM image of (a) Pure ZnO on Si (Z/Si) (b) Au thin film (Au_1.3) (c) 15 nm Au NPs (Au_15) and (d) 40 nm Au NPs mediated ZnO on Si surfaces.

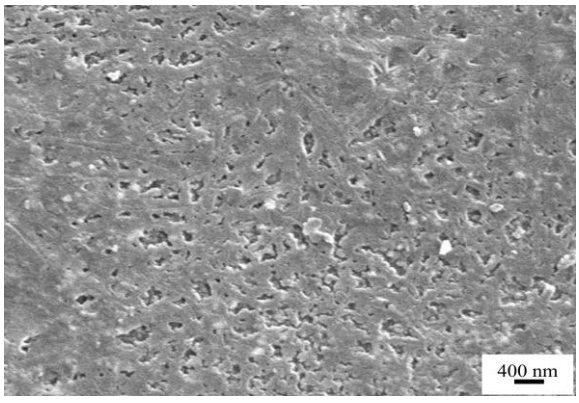

Fig. 6. SEM image of 40 nm Au NPs mediated ZnO growth with Er doped ZA precursor (Au_40Er).

On doping pure ZA precursor solution by Er ions for 40 nm Au NPs mediated ZnO growth by CoSP reactor under same deposition conditions, lower ZnO growth with no ZnO nanorods is observed, which is shown in Fig. 6.

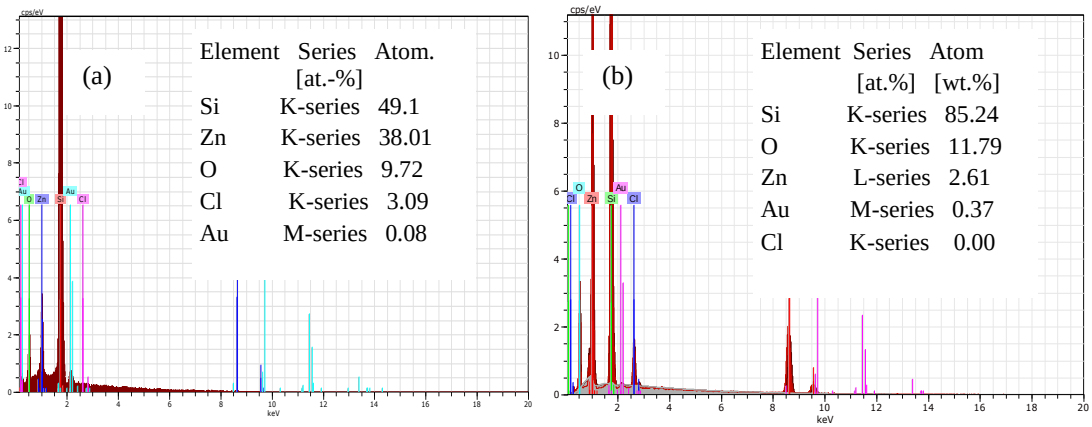

Fig. 7 EDX spectrum of 40 nm Au NPs mediated ZnO growth with (a) pure ZA precursor (Au_40) and (b) Er doped ZA precursor (Au_40).

All ZnO thin film show elemental presence of Au, Zn, Cl and O in Au NPs mediated ZnO growth as shown in Fig. 7 (a) for sample Au_40. The chlorine (Cl) incorporation may be attributed to seed layer solution content. On doping pure ZA precursor by Er ions for sample Au_40Er, EDX spectra depicts considerable reduction of Zn element with lower Zn/O ratio as shown in Fig. 7 (b). The chlorine removal and absence of Er ions for sample Au_40Er may be attributed to appreciable difference in atomic size, charge and atomic weight of Er with respect to Zn [26].

3.4. PL study

ZnO nanostructure thin films have been studied in the wavelength region 370-550 nm through room temperature PL measurement with 325 nm He–Cd laser as the excitation source and the measured PL spectrum is shown in Fig. 8. Almost no emission peak is observed for the case of bare silicon. Since PL measurement for samples Au_40Er and Au_1.3 are same. Therefore PL spectrum of Au_1.3 is representing PL for Au_40Er as well. No emission peaks for ZnO in both Au_1.3 and Au_40Er may be attributed to lower ZnO growth. Relatively high near band edge emission peak of ZnO with respect to the visible emission peak confirm better optical quality of ZnO thin film for samples Au_15 and Au_40. Higher emission properties of ZnO thin film may be attributed to the presence of intrinsic point defects. The sample Z/Si show absence of 520 nm PL peak as compare to Au NPs mediated PL spectrum and additional PL peaks around 550 nm for interstitial oxygen defect [27] is observed.

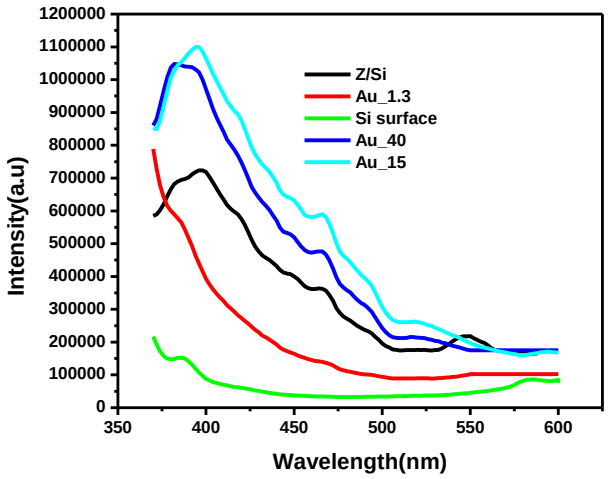

Fig.8 PL spectrum of bare Si substrate and gold mediated ZnO thin films

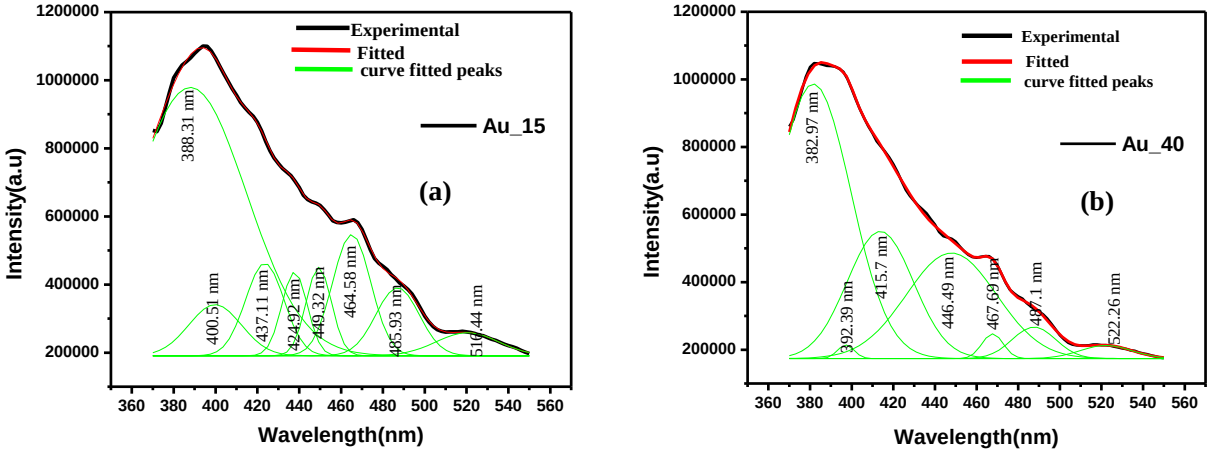

Fig. 9. Gaussian fitted PL peaks for (a) 15 nm (Au_15) and (b) 40 nm (Au_40) Au particles mediated ZnO growth.

To study size dependent optical changes in Au NPs mediated ZnO growth, two corresponding PL spectrums are Gaussian deconvoluted to the subpeaks according to their origin as shown in Fig. 6. If Au NPs size is increased, a blue shift of excitonic peak [28] in ZnO growth is observed. Donor related emission peak at 392, 400.5 and 415.7 nm [29-31] are observed for defects such as Zinc interstitial (Zn_i) with relatively higher concentration for sample Au_40. Acceptor related emission peaks at 424.9, 464.58 and 467.69 nm [32-33] for interstitial oxygen defect (O_i) is found to be red shifted and quenched for sample Au_40. The emission peak at 437.11, 446.49 and 449.32 nm may be attributed to the presence of surface defects [34-35], which suggest larger number of surface defect for the case of 15 nm Au NPs mediated ZnO growth (Au_15). The emission peaks at around 485 nm and 520 nm may be attributed to vacancy of oxygen (V_o) and antisite oxygen defect (O_{Zn}) [36-37]. Thus, overall less defect peaks and higher donor related peaks are observed for 40 nm Au NPs mediated ZnO growth which suggests possibility of size dependent electrical and optical behaviour of ZnO nanostructure layers mediated by Au NPs in this CoSP reactor.

3.5. Reflection study

Reflectance spectrums for Au thin film, Au NPs layer on Si and Au NPs, Au thin film mediated ZnO growths on Si surface are shown in Fig. 10. The reflection spectrum in Fig. 10 (a) clearly confirms that a higher absorption is observed for the case of 40 nm Au NPs on Si surface. On comparing light reflectance of Au thin film (Au_film/Si) and Au NPs on Si surface with respect to polished Si surface, relatively higher absorption is observed ~500 nm wavelength region (Fig. 10 (a) and Fig. 10 (b)) for Au film or NPs which may be attributed to surface plasmon effect of Au material. In the case of Au NPs supported ZnO growth, relatively higher LSPR is observed for 40 nm Au NPs mediated ZnO growth (Au_40). For Au thin film mediated ZnO growth, the light reflectance appreciably goes down to nearly 15 % from 61% in the wavelength region 300-1200 nm due to ZnO deposition by CoSP reactor with no characteristic ZnO absorption behavior in the spectrum. The constant absorption band edge for ZnO is clearly visible in the reflection spectrum for all the ZnO films except Au_1.3 and Au_40Er, which may be attributed to lower ZnO growth. The multibranched ZnO nanorod surface morphology for sample Z/Si does not change reflection appreciably on Si surface. But in the case of Au NPs mediated ZnO growth, reduced light reflectance is appreciable. The average reflectance value in 300 – 1200 nm wavelength regions for Si surface, Z/Si, Au_15, Au_40 and Au_40Er are 41.4, 32.01, 21.2, 18.7 and 27.6 % respectively. Thus, there is a reduction of nearly 54.6% of existing reflectance for Au_40, which can be attributed to the combination of ZnO nanostructure formation and increased LSPR. But relatively lower light reduction is observed in 40 nm Au NPs mediated ZnO growth for the case of Er doped ZA precursor (Au_40Er) due to lower ZnO growth.

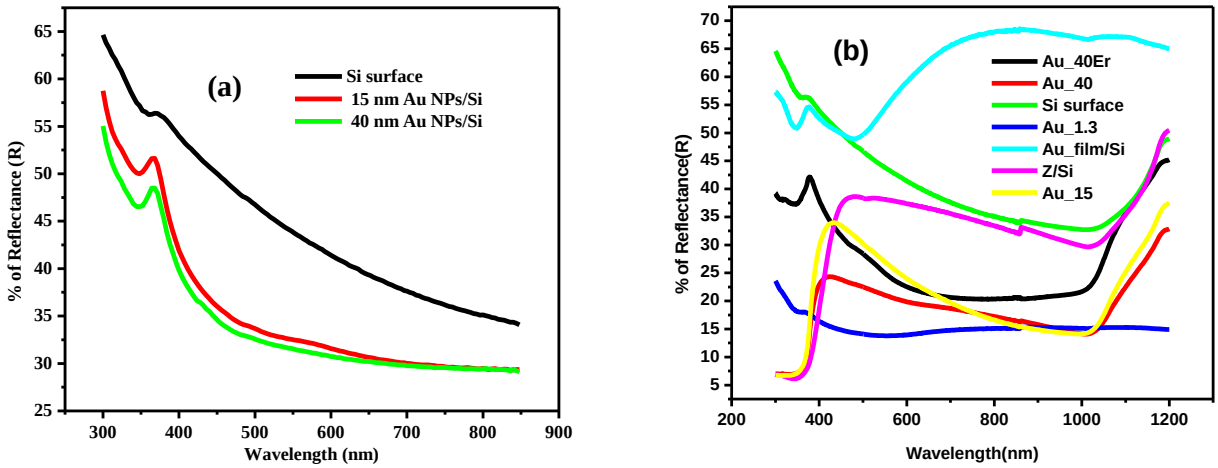

Fig. 10. Reflectance of (a) Au NPs on Si (b)15 nm (Au_15), 40 nm (Au_40, Au_40Er) Au NPs and Au thin film (Au_1.3) mediated ZnO growth on Si.

4. Conclusions

This work shows the role of Au NPs and thin film in the growth of ZnO nanostructure layer on Si surface by CoSP reactor for optical enhancement. Though XRD measurement couldn't detect Au peaks in ZnO thin film but (002) oriented growth in ZnO deposition is observed for the case of Au_15. While extra Au fcc peaks are observed for samples Au_40 and Au_40Er. This size dependent Au NPs ZnO growth can be attributed to the fact that the Au NPs melting temperature reduces with their sizes on Si substrate [38-39] and accordingly they behave differently during ZnO deposition in CoSP reactor. Therefore it can be predicted that for 15 nm Au NPs mediated ZnO growth, particles are melted while 40 nm Au NPs remained in solid form during ZnO deposition. Reflectance measurements confirm noticeable fall of 54.6 and 48.8% of existing reflectance in 300-1200 nm wavelength regions for Au_40 and Au_15. The coalescence amongst nanorods, nanostructure density, Si

surface area coverage and LSPR effect are increased in ZnO growth with the sizes of Au NPs. Au thin film supported ZnO growth confirms remarkable light suppression upto 75% of existing reflectance compared to bare Au thin film onto Si surface. The PL measurement reveals that optical properties of Au NPs mediated ZnO thin film is size dependent and less defects related emission peaks are observed for larger size Au NPs. This growth of nanostructure layer comprising ZnO nanorods and Au NPs can be achieved in roll to roll deposition by CoSP reactor and can be easily integrated in the existing Si solar cell fabrication line. The addition of Er ions in precursor solution with the presence 40 nm Au NPs on Si surface helps in removing chlorine impurity in ZnO thin film with lower ZnO growth. These ZnO nanostructure layers can be further tuned for the increase in photocurrent and photoabsorption of Si solar cell by changing parameters such as size, density of Au particles under various deposition parameters of the CoSP reactor.

References

[1] J. John, V.Prajapati, B. Vermang, A. Lorenz, C. Allebe, A. Rothschild, L. Tous, A. Uruena, K. Baert, J. Poortmans, EPJ Photovoltaic, **3**, 35005 (2012).

[2] M.A. Green, Silicon Solar Cells: Advanced Principles and Practice (Bridge Printer, Sydney, 1995.

[3] Y.T. Cheng, J.J. Ho, S.Y, Tsai, Z.Z. Ye, W. Lee, D.S. Hwang, S. H. Chang, C.C. Chang, W.L. Wang, Solar Energy, **85,** 87 (2011).

[4] C. Yang, G. Zhang, H.M. Li, W.J. Yoo, Journal of Korean Physical Society **56**(5), 1488 (2010).

[5] D.M. Schaadt, B. Feng, E.T. Yu, Applied Physics Letters **86,** 063106 (2005).

[6] U. Kreibig, M. Vollmer, Optical properties of metal clusters, Springer, Germany, 1995.

[7] C.F. Bohren, D.R. Huffmen, Absorption and scattering by small particles, Wiley intersceince, New York, p. 57180, 1983.

[8] C.C. Chang , N.F. Chiu, D.S. Lin, S.Y. Chu, Y.H. Liang, C.W. Lin, Analytical Chemistry, **82**(4), 1207 (2010).

[9] Y.C. Tu, T.Y. Huang, Sensors (Basel), **14**(1), 170 (2014).

[10] T. Singh, D.K. Pandya, R. Singh, Thin Solid Films, **520**(14), 4646 **(**2012).

[11] T. Singh, D.K. Pandya, R. Singh, Journal of Alloys and Compounds, **552,** 294 **(**2013).

[12] J.Y. Chenand, K.W. Sun, Solar Energy Materials Solar Cells, **94,** 930 (2010).

[13] Y. J. Lee, D.S. Ruby, D.W. Peters, B.B. McKenzie, J.W.P. Hsu, Nanoletters, **8**(5), 1501 (2008).

[14] A. Pantea, D. Olgu, E. Firat, T. Rasit, E.U. Husnu, Journal of American Ceramic Society, **96**(4), 1253 (2013).

[15] Y. Xuegong, W. Dong, Dong Li, Genhu Li, Y. Deren, Nanoscale Research Letters, **7,** 306 (2012).

[16] V. Dutta, H. Dhasmana, C. Dwivedi, XVth International workshop on physics of semiconductor devices, JMI, New Delhi India, p. 947, 2009.

[17] H. Verma, D. Mukherjee, S. Witanachchi, P. Mukherjee, M. Batzill, Journal of Crystal Growth, **312,** 2012 (2010).

[18] K. S. Kim, H.W. Kim, Physica B, **328,** 368 (2003).

[19] V. Dutta, C. Dwivedi, Process for making nanorods of Zinc Oxide and resulting products thereof, Patent Application Filed: 2163/DEL/2010.

[20] D.L. Guo, X. Huang, G.Z. Xing, Z. Zhang, G.P. Li, Hi Me, Hua Zhang, Hongyu Chen, Tom Wu., Physical Review B, **83,** 045403 (2011).

[21] Y.F. Chan, H.J. Xu, L. Cao, Y. Tang, D.Y. Li, Journal of Applied Physics, **111,** 033104 (2012).

[22] Y. Zhang, G. Sun, H. Zhao, J. Li, Z. Zheng, Physica Scripta, **84,** 045402 (2011).

[23] G. Zhang, A. Nakamura, T. Aoki, J. Temmyo, Y. Matsui, Applied Physics Letters, **89,** 113112 (2006).

[24] Wei Bai , K.L. Choy , N.H.J. Stelzer , J. Schoonman, Solid State Ionics, **116**, 225 (1999).

[25] N.N. Long, L.V. Vu, C.D. Kiem, S.C. Doanh, C.T. Nguyet, P.T. Hang, Journal of Physics: Conference Series, **187,** 012026 (2009).

[26] X. Zeng, J. Yuan, L. Zhang, Journal Physical Chemistry C, **112,** 3503 (2008).

[27] X.M. Fan, J.S. Lian, Z.X. Guo, H.J. Lu, 2005 Applied Surface Science **239,** 176 (2008).

[28] U. Ozgur, Y.I. Alivov, C. Liu, A. Teke, M.A. Reshchikov, S. Dogan, V. Avrutin, S.J. Cho, H. Morkoc, Journal of Applied Physics, **98,** 041301 (2005).

[29] E.G. Bylander, Journal Applied Physics, **49,** 1188 (1978).

[30] N. Han, P. Hu, A.H. Zuo, D.W. Zhang, Y.J. Tian, Y.F. Chen, Sensors and Actuators B: Chemical, **145**, 114 (2010).

[31] A.H. Zeng, G. Duan, Y. Li, S. Yang, X. Xu, W. Cai, Advanced Functional Materials, **20,** 561 (2010).

[32] S. Sali, M. Boumaour, M. Kechouane, S. Kermadi, F. Aitamar, Physica B, **407,** 2626 (2012).

[33] X.L. Wu, G.G. Siu, C.L. Fu, H.C. Ong, Applied Physics Letters, **78,** 2285 (2001).

[34] A.J. Reddy, M.K. Kokila, H. Nagabhushana, J.L. Rao, C. Shivakumara, B.M. Nagabhushana, R.P. Chakradhar, Spectrochim Acta Part A Molecular Biomolecular Spectroscopy, **81,** 59 (2011).

[35] H. Zeng, G. Duan, Y. Li, S. Yang, X. Xu, W. Cai, Advanced Functional Materials, **20,** 561 (2010).

[36] W. Cheng, P. Wu, X. Zou, T. Xiao, Journal of Applied Physics, **100,** 054311 (2006).

[37] T.M. Borseth, B.G. Svensson, A.Y. Kuznetsov, P. Klason, Q.X. Zhao, M. Willander, Applied Physics Letters, **89,** 262112 (2006).

[38] A. Safaei, Journal of Physical Chemistry C, **114** 13482 (2010).

[39] W. Luo, K. Su, K. Li, G. Liao, N. Hu, M. Jia, Journal of Chemical Physics, **234,** 704 (2012).

Corresponding author: hrishikeshd07@gmail.com